Control of unstable steady states by time-delayed feedback methods

P. Hövel* and E. Schöll
Institut für Theoretische Physik, TU Berlin, Hardenbergstraße 36, D-10623 Berlin, Germany
(Received 25 April 2005; published 4 October 2005)

We show that time-delayed feedback methods, which have successfully been used to control unstable periodic orbits, provide a tool to stabilize unstable steady states. We present an analytical investigation of the feedback scheme using the Lambert function and discuss effects of both a low-pass filter included in the control loop and nonzero latency times associated with the generation and injection of the feedback signal.

DOI: 10.1103/PhysRevE.72.046203 PACS number(s): 05.45.Gg, 02.30.Ks

I. INTRODUCTION

Starting with the work of Ott, Grebogi, and Yorke [1] a variety of methods for controlling unstable and chaotic systems have been developed in the last 15 years and applied to various real systems in physics, chemistry, biology, and medicine [2–4]. Pyragas [5] introduced a time-delayed feedback scheme that stabilizes unstable periodic orbits (UPOs) embedded in a chaotic attractor by constructing a control force from the difference of the current state to the state one period in the past. This method is known as *time-delay autosynchronization* (TDAS) and was improved by Socolar *et al.* [6] by considering multiple delays in form of an infinite series (*extended TDAS* or ETDAS) or an average of N past iterates (*N time delay autosynchronization* or NTDAS) [7] or coupling matrices (*generalized ETDAS* or GETDAS) [8]. In parallel to the control of UPOs, the stabilization of unstable steady states (USSs) became a field of increasing interest.

One of the methods to control an USS introduced by Bielawski *et al.* uses the derivative of the current state as source of a control force [9]. It can be shown, however, that this *derivative control* is sensitive to high frequency oscillations [10] and thus not robust in the presence of noise. Another control scheme was given by calculating the difference of the current state to a low-pass filtered version [11].

Although the effects of time-delayed feedback schemes on the stability of periodic orbits are understood to a large extent [12–16], much less is known in the case of a fixed point. There are some results discussing the application of the ETDAS control method [17] and numerical simulations of Chua's circuit [18], but a detailed theoretical investigation is still missing.

The purpose of this paper is the analytical and numerical study of the TDAS method, which was originally invented to control unstable periodic orbits [5], in application to unstable fixed points, including latency and filtering effects. The paper is organized as follows. In Sec. II we will introduce the system's equations and the control force. In Sec. III we will investigate the domain of control in dependence on time delay and feedback gain and present analytical solutions of the characteristic equation using the Lambert function. Further, we will consider the effects of nonzero latency times and additional low-pass filtering in Secs. IV and V, respectively.

II. CONTROL BY TIME-DELAYED FEEDBACK

We consider a general dynamic system given by a vector field $\mathbf{f}$:

$$\dot{\mathbf{x}} = \mathbf{f}(\mathbf{x}) \tag{1}$$

with an unstable fixed point $\mathbf{x}^*$ given by $\mathbf{f}(\mathbf{x}^*)=\mathbf{0}$. The stability of this fixed point is obtained by linearizing the vector field around $\mathbf{x}^*$. Without loss of generality, let us assume $\mathbf{x}^*=0$. In the following we will consider the generic case of an unstable focus for which the linearized equations in center manifold coordinates x,y can be written as

$$\dot{x} = \lambda x + \omega y, \tag{2}$$

$$\dot{y} = -\omega x + \lambda y,$$

where λ and ω are positive real numbers. They may be viewed as parameters governing the distance from the instability threshold, e.g., a Hopf bifurcation of system (1), and the intrinsic eigenfrequency, respectively. For notational convenience, Eq. (2) can be rewritten as

$$\dot{\mathbf{x}}(t) = \mathbf{A}\mathbf{x}(t). \tag{3}$$

The eigenvalues Λ_0 of the matrix $\mathbf{A}$ are given by $\Lambda_0 = \lambda \pm i\omega$, so that for $\lambda > 0$ and $\omega \neq 0$ the fixed point is indeed an unstable focus. A vanishing imaginary part, i.e., $\omega=0$, would correspond—in the case of a UPO—to an orbit without torsion for which TDAS fails [12]. We note that the same holds for USSs and therefore we restrict our investigation to $\omega \neq 0$.

We shall now apply time-delayed feedback control [5] in order to stabilize this fixed point:

$$\dot{x}(t) = \lambda x(t) + \omega y(t) - K[x(t) - x(t-\tau)], \tag{4}$$

$$\dot{y}(t) = -\omega x(t) + \lambda y(t) - K[y(t) - y(t-\tau)],$$

where the feedback gain K and the time delay τ are real numbers. The goal of the control method is to change the sign of the real part of the eigenvalue.

Since the control force applied to the ith component of the system involves only the same component, this control

*Electronic address: phoevel@physik.tu-berlin.de

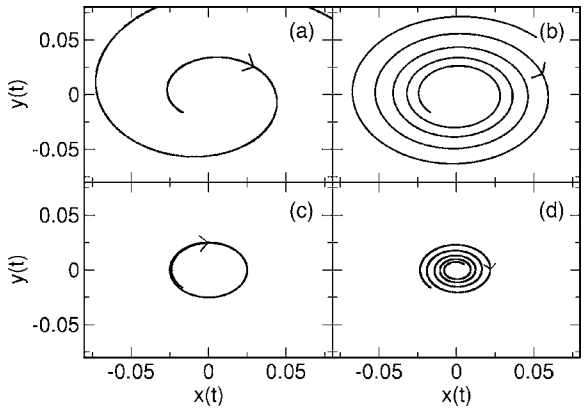

FIG. 1. Control of an unstable focus with $\lambda=0.5$ and $\omega=\pi$ in the configuration space for different values of the feedback gain K. Panels (a)–(d) correspond to $K=0,0.2,0.25$, and 0.3, respectively. The time delay τ of the TDAS control scheme is chosen as 1, corresponding to $\tau=T_0/2=\pi/\omega$.

scheme is called diagonal coupling [19], which is suitable for an analytical treatment. Note that the feedback term vanishes if the USS is stabilized since $x^*(t-\tau)=x^*(t)$ and $y^*(t-\tau)=y^*(t)$ for all t, indicating the noninvasiveness of the TDAS method.

Figure 1 depicts the dynamics of the controlled unstable focus ($\lambda=0.5$ and $\omega=\pi$) in the $x-y$ plane for different values of the feedback gain K. Panels (a)–(d) correspond to increasing K. The time delay of the TDAS control scheme is chosen as $\tau=1$ in all panels. Panel (a) displays the case of the absence of control, i.e., $K=0$, and shows that the system is an unstable focus exhibiting undamped oscillations on a time scale $T_0\equiv 2\pi/\omega=2$. It can be seen from panel (b) that increasing K reduces the instability. The system diverges more slowly to infinity indicated by the tighter spiral. Further increase of K stops the unstable behavior completely and produces periodic motion, i.e., a center [see panel (c)]. The amplitude of the orbit depends on the initial conditions, which are chosen as $x=0.01$ and $y=0.01$. For even larger feedback gains, the trajectory becomes an inward spiral and thus approaches the fixed point, i.e., the focus. Hence the TDAS control scheme is successful.

An exponential ansatz for $x(t)$ and $y(t)$ in Eq. (4), i.e., $x(t)\sim\exp(\Lambda t)$, $y(t)\sim\exp(\Lambda t)$, reveals how the control force modifies the eigenvalues of the system. The characteristic equation becomes

$$[\Lambda + K(1-e^{-\Lambda\tau}) - \lambda]^2 + \omega^2 = 0 \tag{5}$$

so that the complex eigenvalues Λ are given in the presence of a control force by the implicit equation

$$\lambda \pm i\omega = \Lambda + K(1-e^{-\Lambda\tau}). \tag{6}$$

Using the Lambert function W, which is defined as the inverse function of $g(z)=ze^z$ for complex z [20–24], Eq. (6) can be solved analytically,

$$\Lambda\tau = W(K\tau e^{-(\lambda\pm i\omega)\tau+K\tau}) + (\lambda\pm i\omega)\tau - K\tau. \tag{7}$$

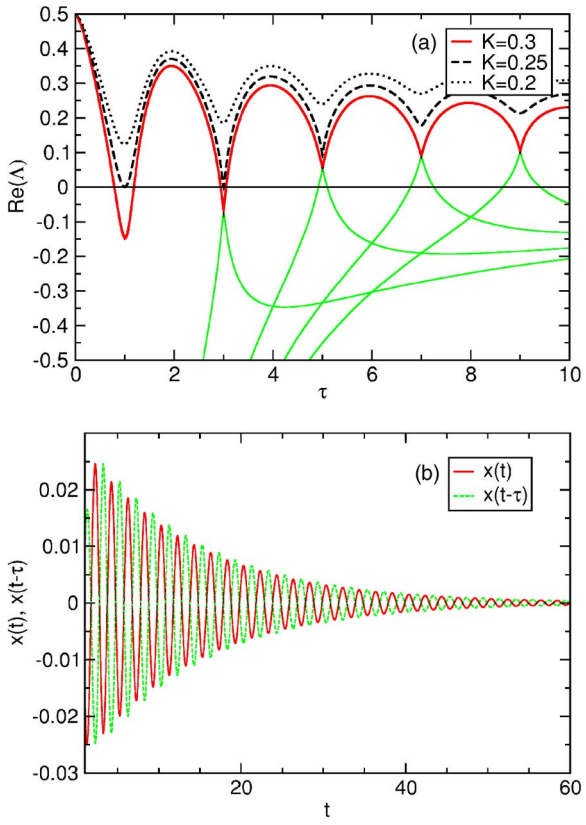

FIG. 2. (Color online) (a) Largest real part of the complex eigenvalues Λ vs τ for $\lambda=0.5$ and $\omega=\pi$ for different K. Some lower eigenvalues are also displayed for $K=0.3$ (green online). (b) Time series of the x component of the unstable focus: The solid line (red online) corresponds to $x(t)$, the dashed line (green online) to the delayed x component $x(t-\tau)$ with $\tau=1$. The parameters of the unstable focus and the control scheme are as in panel (d) of Fig. 1.

Panel (a) of Fig. 2 shows the dependence of the largest real part of the complex eigenvalues Λ upon the time delay τ according to Eqs. (6) and (7) for $\lambda=0.5$ and $\omega=\pi$. The solid curve corresponds to a feedback gain of $K=0.3$, the dashed curve to $K=0.25$, and the dotted curve to $K=0.2$. All curves start at $\mathrm{Re}(\Lambda)=\lambda$ for $\tau=0$, i.e., when no control is applied to the system. For increasing time delay, the real part $\mathrm{Re}(\Lambda)$ decreases. It can be seen in the case of $K=0.3$ that there exist values of the time delay for which $\mathrm{Re}(\Lambda)$ becomes negative, and thus the control is successful. The curve for $K=0.25$ shows the threshold case where $\mathrm{Re}(\Lambda)$ becomes zero for $\tau=1$, but does not change sign. The TDAS control scheme generates an infinite number of additional eigenmodes. The corresponding eigenvalues are the solutions of the transcendental Eq. (6). The real parts of the eigenvalues all originate from $-\infty$ for $\tau=0$. Some of these lower eigenvalues are displayed for $K=0.3$. The different branches of the eigenvalue spectrum originate from the multiple-leaf structure of the complex Lambert function. The real part of each eigenvalue branch exhibits a typical nonmonotonic dependence upon τ which leads to crossover of different branches resulting in an oscillatory modulation of the largest real part as a function of τ. Such behavior of the eigenvalue spectrum appears to be quite general, and has been found for various delayed feed-

back coupling schemes, including the Floquet spectrum of UPOs [19,26] and applications to noise-induced motion where the fixed point is stable [27].

The notch at $\tau=1$ corresponds to Fig. 1, so that at this value of τ the solid, dashed, and dotted curves correspond to panels (d), (c), and (b) of Fig. 1, respectively. The notches at larger τ become less pronounced leading to less effective realization of the TDAS control scheme, i.e., a smaller or no τ interval with negative $\mathrm{Re}(\Lambda)$.

In the case of an UPO the optimal time delay is equal to the period of the orbit to be stabilized. Note that in the case of an USS, however, the time delay is not so obviously related to a parameter of the system. We will see in Sec. III which combinations of the feedback gain K and the time delay τ lead to successful control.

Panel (b) of Fig. 2 displays the time evolution of $x(t)$ and its time-delayed counterpart $x(t-\tau)$ in the case of a combination of $K=0.3$ and $\tau=1$ that leads to successul control as in panel (d) of Fig. 1. The x component of the control force can be calculated from the difference of the two curves and subsequent multiplication by K. Since $x(t)$ tends to zero in the limit of large t (the system reaches the focus located at the origin), the control force vanishes if the system is stabilized. Thus the control scheme is noninvasive. Note that the current signal (red online) and its delayed counterpart (green online) are in antiphase. This observation will become important in Sec. IV.

In the following discussion, it is helpful to consider the real and imaginary part of Eq. (6) separately in order to gain some analytic information about the domain of control:

$$p + K[1 - e^{-p\tau}\cos(q\tau)] = \lambda, \tag{8}$$

$$q + Ke^{-p\tau}\sin(q\tau) = \omega$$

with $\Lambda=p+iq$.

III. SHAPE OF THE DOMAIN OF CONTROL

This section is focused on the construction of the domain of control in the $K-\tau$ plane. The calculation can be done analytically for special points by using, for instance, that $p=0$ at the threshold of control. Furthermore, we will present an expansion around the minimal value of K that reveals further details of the shape of the domain of control.

At the threshold of control the sign of the real part p of the exponent Λ changes. Therefore setting p to zero in the real and imaginary parts, respectively, of Eq. (8) yields

$$\lambda = K[1 - \cos(q\tau)] \tag{9}$$

and

$$\omega = q + K\sin(q\tau). \tag{10}$$

Since the cosine is bounded between -1 and 1, the following inequality follows from Eq. (9):

$$\frac{\lambda}{2} \leqslant K. \tag{11}$$

Thus a minimal value of K, $K_{\min}=\lambda/2$, for which the control starts, can be inferred [25]. It corresponds to $q\tau=(2n+1)\pi$ for $n=0, 1, 2,\ldots$.

In order to express the values of the time delay τ that correspond to the minimal K in terms of the parameters of the uncontrolled system, it is useful to consider even and odd multiples of π for $q\tau$, i.e., $q\tau=2n\pi$ and $q\tau=(2n+1)\pi$ for $n=0, 1, 2,\ldots$. In both cases, the imaginary part of Eq. (6) leads to $q=\omega$. Hence, in the latter case, the time delay τ for $K_{\min}=\lambda/2$ becomes

$$\tau = \frac{\pi}{\omega}(2n+1). \tag{12}$$

The last expression can be rewritten using the uncontrolled eigenperiod T_0,

$$\tau = T_0\frac{2n+1}{2}, \tag{13}$$

where T_0 is defined by

$$T_0 = \frac{2\pi}{\omega}. \tag{14}$$

This discussion has shown that $K=\lambda/2$ and $\tau=T_0(2n+1)/2$ with $n=0, 1, 2,\ldots$ correspond to points of successful control in the $K-\tau$ plane with minimal feedback gain.

For even multiples, i.e., $q\tau=2n\pi$ for $n=0, 1, 2,\ldots$, no control is possible for finite values of K, since

$$\frac{K-\lambda}{K} = \cos(q\tau)\Big|_{q\tau=2n\pi} \tag{15}$$

$$\Leftrightarrow 1 - \frac{\lambda}{K} = 1, \tag{16}$$

which cannot be satisfied for $\lambda \neq 0$ and finite K. Furthermore, Eq. (10) yields that for time delays, which are integer multiples of the eigenperiod, i.e., $\tau=T_0 n=2\pi n/\omega$ with $n=0, 1, 2,\ldots$, the control scheme fails for any feedback gain. Note that this failure appears to be related to the case of torsion-free UPOs, where it has been shown that $\omega\neq 0$ is a necessary condition for control [12].

Another result that can be derived from Eq. (6) is a shift of q for increasing K. For this, taking the square of the real and imaginary part of Eq. (6) and using trigonometrical identities yields

$$q = \omega \mp \sqrt{(2K-\lambda)\lambda}. \tag{17}$$

Inserting Eq. (17) into the real part of Eq. (6) leads to an explicit expression for the dependence of time delay τ on the feedback gain K at the threshold of stability, i.e., the boundary of the control domain $p=0$,

$$\frac{K-\lambda}{K} = \cos(q\tau) \tag{18}$$

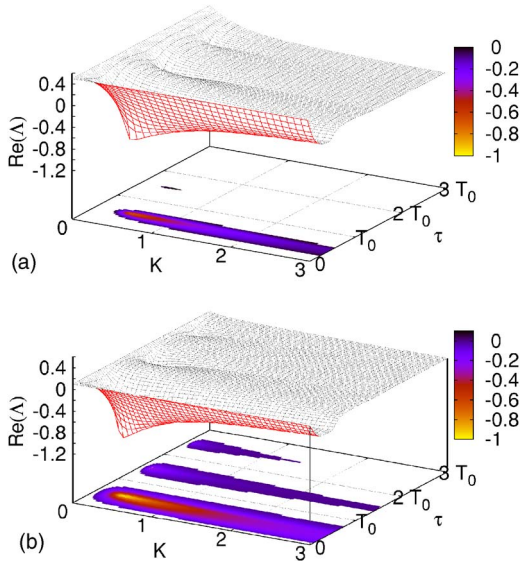

FIG. 3. (Color online) Domain of control in the K-τ plane and largest real part of the complex eigenvalues Λ as a function of K and τ according to Eq. (7). The two-dimensional projection at the bottom shows combinations of τ and K, for which Re(Λ) is negative and thus the control successful [panel (a): $\lambda=0.5$ and $\omega=\pi$; panel (b): $\lambda=0.1$ and $\omega=\pi$].

$$\Leftrightarrow \tau(K) = \frac{\arccos\left(\frac{K-\lambda}{K}\right)}{\omega \mp \sqrt{(2K-\lambda)\lambda}}. \tag{19}$$

In order to visualize the shape of the domain of control we will investigate how small deviations $\epsilon>0$ from $K_{\min}$, i.e, $K=\lambda/2+\epsilon$, influence the corresponding values of the time delay τ. For this, let $\eta>0$ be small and $\tau=(\pi/\omega)(2n+1)\pm\eta$ a small deviation from τ at $K_{\min}$. Inserting the expression for K and τ into Eq. (18) yields after some Taylor's expansions

$$-1+\frac{4}{\lambda}\epsilon = -1+\frac{1}{2}\left[\omega\eta \mp \frac{\pi}{\omega}(2n+1)\sqrt{2\lambda}\sqrt{\epsilon}\right]^2 \tag{20}$$

$$\Leftrightarrow \eta = \left[\pm\frac{2\sqrt{2}}{\omega\sqrt{\lambda}} + \frac{\sqrt{2}\pi}{\omega^2}(2n+1)\sqrt{\lambda}\right]\sqrt{\epsilon}. \tag{21}$$

This equation describes the shape of the domain of control at the threshold of stabilization, i.e., $p=0$, near the minimum K value at $\tau=T_0(2n+1)/2$ in the $K-\tau$ control plane. Small deviations from τ at $K_{\min}$ are influenced by the square root of small deviations from the minimum feedback gain.

Figure 3 displays the largest real part of the eigenvalues Λ in dependence on both the feedback gain K and the time delay τ for $\omega=\pi$ and two different values of λ, and summarizes the results of this section. The values of Λ are calculated using the analytic solution (7) of Eq. (6). The two-dimensional projections at the bottom of each plot extract combinations of K and τ with negative p, i.e., successful control of the system. In the absence of a control force, i.e., $K=0$, the real part of Λ starts at λ. Increasing the feedback gain decreases Re(Λ). For $K=K_{\min}=\lambda/2$, the real part of the eigenvalue reaches 0 for certain time delays, i.e., $\tau=T_0(2n+1)/2$ with $n=0, 1, 2,\ldots$, and then changes sign. Thus the system is stabilized. For values of the feedback gain slighty above the minimum value $K_{\min}$, the domain of control shows a square root shape. It can be seen that for time delays of $\tau=T_0 n$ the largest real part of the eigenvalues remains positive for any feedback gain. For a smaller value of λ [Fig. 3(b)], i.e., closer to the instability threshold of the fixed point, the domains of control become larger.

An example of the combination of minimal feedback gain $K_{\min}=\lambda/2$ and corresponding time delay $\tau=T_0(2n+1)/2$, $n=0, 1, 2,\ldots$ is shown in panel (c) of Fig. 1, where $K=\lambda/2=0.25$ and $\tau=T_0/2=\pi/\omega=1$. It describes the control threshold case between stable and unstable fixed point.

IV. LATENCY TIME EFFECTS

In this section we will consider nonzero latency times, which can be associated with the generation and injection of the feedback signal [28]. It has been shown experimentally [29] in the case of an UPO that latency can have important effects on the controllability of the system and might limit the success of the time-delayed feedback method. A theoretical explanation can be found in Refs. [30,31]. Here we will discuss how latency times change the domain of control in the case of an USS.

The latency time δ can be included as an additional time delay in the control force of Eq. (4), which then becomes

$$\mathbf{F}(t-\delta) = -K\begin{pmatrix} x(t-\delta)-x(t-\tau-\delta) \\ y(t-\delta)-y(t-\tau-\delta)\end{pmatrix}, \tag{22}$$

leading to a characteristic equation similar to Eq. (6) but with an additional exponential factor

$$\lambda \pm i\omega = \Lambda + Ke^{-\Lambda\delta}(1-e^{-\Lambda\tau}) \tag{23}$$

or, separating into real and imaginary parts,

$$p + K[e^{-p\delta}\cos(q\delta) - e^{-p(\tau+\delta)}\cos(q(\tau+\delta))] = \lambda,$$

$$q - K[e^{-p\delta}\sin(q\delta) - e^{-p(\tau+\delta)}\sin(q(\tau+\delta))] = \omega,$$

where p and q denote the real and imaginary part of Λ, respectively.

Figure 4 displays the dependence of the largest real part of the complex eigenvalues Λ on the time delay τ according to Eq. (23) for $\lambda=0.5$ and $\omega=\pi$, and different values of the latency time δ. The values of the eigenvalues are calculated by solving Eq. (23) numerically. The solid, dashed, dotted, and dash-dotted curves correspond to $\delta=0$, 0.1, 0.2, and 0.3, respectively. The case with zero latency time is also displayed; it corresponds to the solid curve in Fig. 2(a).

It can be seen that increasing latency time shifts the minimum of p to smaller values of τ and reduces the intervals of τ, for which p is negative, i.e., for which the control is successful. The dash-dotted curve ($\delta=0.3$) shows a case where no control is possible since the largest real part of the complex eigenvalues remains positive for all time delays τ.

Solving Eq. (23) analytically by using the Lambert function, as for Eq. (6), is not possible in the case of non-

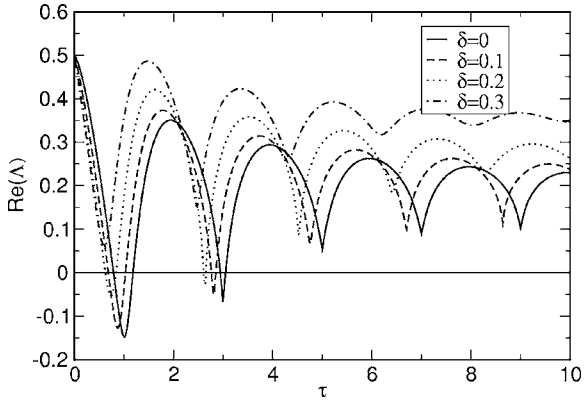

FIG. 4. Largest real part of the eigenvalues Λ vs τ for $\lambda=0.5$, $\omega=\pi$, and $K=0.3$ as given by Eq. (23). The solid, dashed, dotted, and dash-dotted curves correspond to a latency time of $\delta=0$, 0.1, 0.2, and 0.3, respectively.

zero latency times due to the additional exponential term $\exp(-\Lambda\delta)$. In order to understand the effects of nonzero latency times on the value of the minimal feedback gain, we evaluate the real part of Eq. (23) at the threshold of control, i.e., $p=0$. It was shown in Sec. III that K becomes minimal if $q\tau=\pi(2n+1)$ for $n=0$, 1, 2,… [see Eqs. (9) and (11)]. This value of $q\tau$ yields for nonzero latency times

$$K_{\min}(\delta)=\frac{\lambda}{2\cos\left[\pi(2n+1)\dfrac{\delta}{\tau}\right]}\geqslant\frac{\lambda}{2}. \tag{24}$$

This shows that nonzero latency times shift the minimal feedback gain $K_{\min}$, for which the control scheme is successful, to larger values.

The effects of the cosine function in Eq. (24) can be understood by considering Fig. 2(b) and Fig. 5, which shows the dependence of the minimal feedback gain $K_{\min}$ on the latency time for $\lambda=0.5$. Increasing latency time increases the value of $K_{\min}$. If δ becomes larger than half the time delay τ, $K_{\min}$ changes sign and control is possible only for negative K with $K<K_{\min}$ and suitably chosen τ. Note that in Fig. 2 the

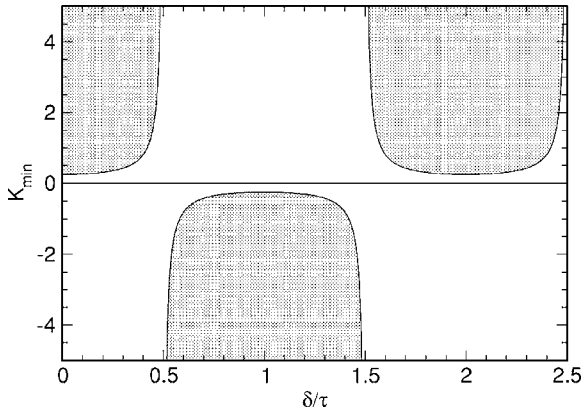

FIG. 5. Minimal feedback gain K vs relative latency δ/τ for $\lambda=0.5$ and $\omega=\pi$ according to Eq. (24). The shaded areas show the domain of control for suitably chosen τ.

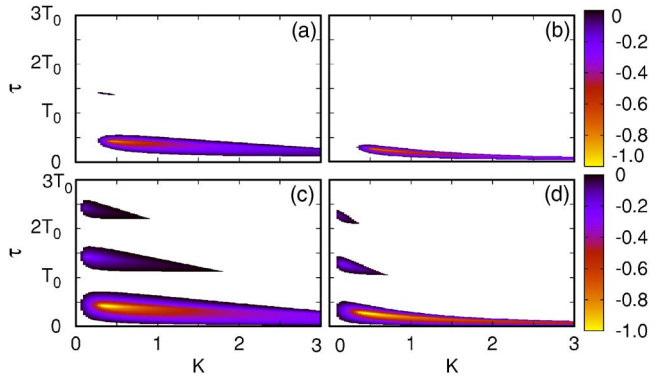

FIG. 6. (Color online) Domain of control in the K-τ plane for different latency times [panels (a) and (c): $\delta=0.1$; panels (b) and (d): $\delta=0.3$]. The shaded areas indicate combinations of τ and K, for which the largest real part of the complex eigenvalues Λ is negative and thus control is successful. The value of $\mathrm{Re}(\Lambda)$ is indicated by the greyscale (color online). The parameters of the unstable focus are chosen as $\omega=\pi$ in all panels and $\lambda=0.5$ in (a) and (b) and $\lambda=0.1$ in (c) and (d).

difference $x(t)-x(t-\tau)$ has to be positive for successful control. For $0.5\tau<\delta<1.5\tau$ both $x(t-\delta)$ and $x(t-\delta-\tau)$ becomes closer to zero. Therefore in order to achieve control, the feedback gain becomes larger. In the limit $\delta/\tau\to1/2$ the difference $x(t-\delta)-x(t-\tau-\delta)$ vanishes and thus the minimal feedback gain diverges. For even larger values of δ the above-mentioned difference changes its sign forcing $K_{\min}$ to do the same. Otherwise the control scheme would generate a force that pulls the system away from the target fixed point.

Figure 6 depicts the domain of control for latency times of $\delta=0.1$ [panels (a) and (c)] and $\delta=0.3$ [panels (b) and (d)]. The largest real part of the complex eigenvalues Λ is shown by greyscale in the domain. It can be seen that increasing latency times reduce the domain of control. For instance, the small range at a time delay of $\tau=1.5T_0$ in (a), where control is possible for $\delta=0.1$, vanishes for $\delta=0.3$ in (b). Note that nonzero latency times lead to a loss of the symmetry [around $\tau=(2n+1)/2T_0$ for $n=1$, 2,…] of the domain of control (see also the case of zero latency as displayed in Fig. 3).

V. LOW-PASS FILTERING

It has been found that high frequency modulations of the control signal, due to additional high frequency components in the signal besides the main frequency, can render the TDAS control method unstable [32]. As shown in that work, an additional low-pass filter included in the control loop can overcome this limitation, and UPOs can be stabilized [32,33]. On the other hand, in electronic signal processing the finite response time of the circuit often imposes unavoidable low-pass filtering, and its effect upon feedback control is not clear. In this section we will show that a low-pass filter changes the characteristic equation [see Eq. (6)] of the fixed point, and shifts the minimal feedback gain to larger values. Note that low-pass filtering has been successfully used to stabilize USSs by generating a control force from the difference of the current state to its filtered counterpart [11].

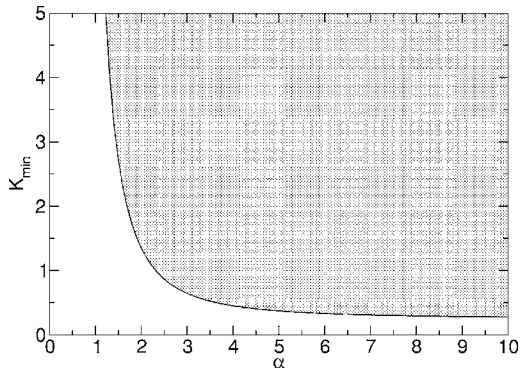

FIG. 7. Minimal feedback gain K vs cutoff frequency α for $\lambda=0.5$ and $\omega=\pi$ according to Eq. (31). The shaded area shows the domain of control.

The TDAS control force with an additional low-pass filter can be written as

$$\mathbf{F}(t) = -K\begin{pmatrix} \bar{x}(t) - \bar{x}(t-\tau) \\ \bar{y}(t) - \bar{y}(t-\tau) \end{pmatrix}, \tag{25}$$

where $\bar{x}$ and $\bar{y}$ denote the filtered versions of x and y defined by

$$\bar{x}(t) = \alpha \int_{-\infty}^{t} x(t') e^{-\alpha(t-t')} dt' \tag{26}$$

with the cutoff frequency α, and analogously for $\bar{y}(t)$. Equivalently, the convolution integrals can be replaced by two additional differential equations such that the original two-dimensional system becomes four-dimensional,

$$\dot{x}(t) = \lambda x(t) + \omega y(t) - K[\bar{x}(t) - \bar{x}(t-\tau)], \tag{27}$$

$$\dot{y}(t) = -\omega x(t) + \lambda y(t) - K[\bar{y}(t) - \bar{y}(t-\tau)],$$

$$\dot{\bar{x}}(t) = -\alpha \bar{x}(t) + \alpha x(t),$$

$$\dot{\bar{y}}(t) = -\alpha \bar{y}(t) + \alpha y(t).$$

This system of differential equations yields a characteristic equation of the form

$$\pm i(\alpha + \Lambda)\omega = \alpha K(1 - e^{-\Lambda\tau}) - (\alpha + \Lambda)(\lambda - \Lambda) \tag{28}$$

or, equivalently, using $\Lambda = p + iq$,

$$\alpha(\lambda - p) = \alpha K[1 - e^{-p\tau}\cos(q\tau)] - q(q - \omega), \tag{29}$$

$$\alpha(\omega - q) = \alpha K e^{-p\tau}\sin(q\tau) - \lambda q - p\omega.$$

Note that in the limit of large cutoff frequencies, i.e., $\alpha \to \infty$, Eqs. (28) and (29) reduce to the characteristic equations (6) and (8) of Sec. II, respectively.

For further investigation of Eq. (28) we shall use the separation into real and imaginary parts (29). Following the discussion of Sec. III by considering even and odd multiples of π as special values for $q\tau$, we obtain from the imaginary part of Eq. (28) in the case $q\tau = (2n+1)\pi$

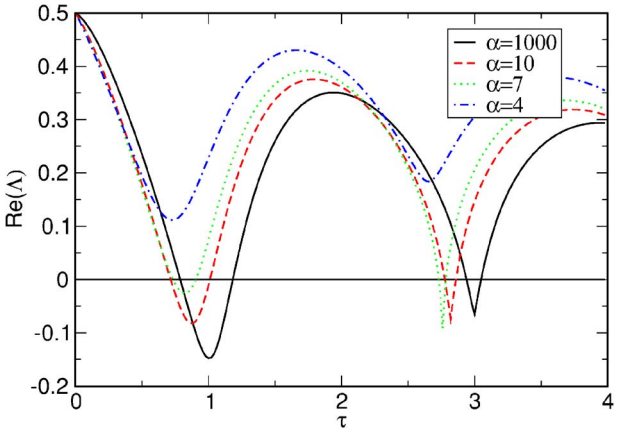

FIG. 8. (Color online) Largest real part of the complex eigenvalues Λ vs τ for $\lambda=0.5$, $\omega=\pi$, and $K=0.3$ as given by Eq. (28). The solid, dashed, dotted, and dash-dotted curves correspond to a cutoff frequency of $\alpha=1000$, 10, 7, and 4, respectively.

$$\tau = \frac{2n+1}{\omega}\pi\left(1 - \frac{\lambda}{\alpha}\right) \tag{30}$$

with $n=0,1,2,\ldots$. Inserting this into the real part of Eq. (28) gives an expression for the minimum value of the feedback gain, for which the control method becomes successful for appropriately chosen τ,

$$K_{\min}(\alpha) = \frac{\lambda}{2} + \frac{\omega^2}{2}\frac{\lambda}{(\alpha - \lambda)^2}. \tag{31}$$

The dependence of the minimal feedback gain $K_{\min}$ on the cutoff frequency α is depicted in Fig. 7 for $\lambda=0.5$ and $\omega=\pi$. For large cutoff frequencies the minimum value tends to the result of Sec. III [see Eq. (11)]. Note that for finite α the minimal feedback gain is shifted to larger values compared to the case of the original TDAS control scheme.

Figure 8 shows the largest real part of the eigenvalues Λ

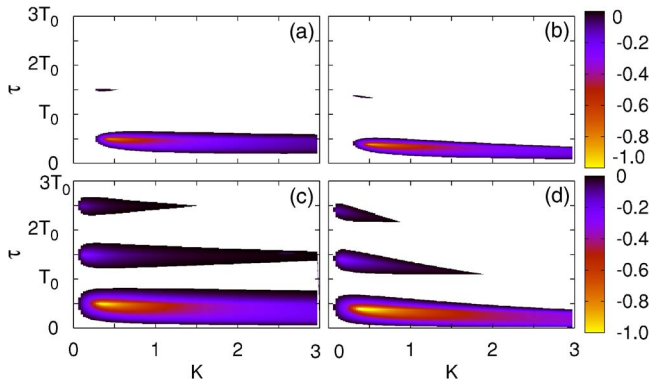

FIG. 9. (Color online) Domain of control in the K-τ plane for different cutoff frequencies [panels (a) and (c): $\alpha=1000$; panels (b) and (d): $\alpha=7$]. The shaded areas indicate combinations of τ and K, for which the largest real part of the complex eigenvalues Λ is negative and thus control is successful. The value of $\mathrm{Re}(\Lambda)$ is indicated by the greyscale (color online). The parameters of the unstable focus are chosen as $\omega=\pi$ in all panels and $\lambda=0.5$ in (a) and (b) and $\lambda=0.1$ in (c) and (d).

in dependence on the time delay τ for fixed feedback gain $K=0.3$ and various cutoff frequencies $\alpha=1000$, 10, 7, and 4. For a large cutoff frequency, i.e., $\alpha=1000$, the curve is similar to the case without low-pass filter [see Fig. 2(a)] indicating that the filter has only little effect. For smaller α, however, filtering the control signal reduces the range of the time delay τ, for which $\mathrm{Re}(\Lambda)$ becomes negative, eventually leading to a complete failure of stabilization. Note that the notches are shifted to lower values of τ for decreasing α. This effect can also be understood by Eq. (30) due to the additional factor $(1-\lambda/\alpha)<1$. The corresponding domains of control in the $K-\tau$ plane are shifted to smaller values of τ and distorted asymmetrically (Fig. 9).

VI. CONCLUSION

We have discussed the effects of time-delayed feedback control upon the stability of steady states. We have computed the domain of stabilization of an unstable focus in the plane parametrized by feedback gain and time delay. Using the complex multivalued Lambert function, we have derived analytically the main features of the stability domain by investigating the characteristic equation of the fixed point. Below a minimum value of the feedback gain no control is possible. In the vicinity of this minimum value, the shape of the domain of control shows a square root dependence on the feedback gain. We find that no control is possible for time delays that are multiples of the uncontrolled eigenperiod of the system. Taking nonzero control loop latencies into account, we have shown that increasing latency times increase the minimum value of the feedback gain K_{min} and reduce the domain of control substantially. Similarily, an additional low-pass filter in the control loop causes a shift of K_{min}, as well. This suggests that filtering with a cutoff frequency α has a similar effect as a latency delay time α^{-1}. In fact, expanding Eq. (24) for small latency δ in lowest order yields the same minimal feedback gain K_{min} as for low-pass filtering (31), if Eq. (30) is observed.

ACKNOWLEDGMENT

This work was supported by Deutsche Forschungsgemeinschaft in the framework of Sfb 555. We are indebted to Andreas Amann and Wolfram Just for stimulating discussions.

[1] E. Ott, C. Grebogi and J. A. Yorke, Phys. Rev. Lett. **64**, 1196 (1990).
[2] H. G. Schuster, *Handbook of Chaos Control* (Wiley-VCH, Weinheim, 1999).
[3] S. Boccaletti, C. Grebogi, Y. C. Lai, H. Mancini, and D. Maza, Phys. Rep. **329**, 103 (2000).
[4] D. Gauthier, G. M. Hall, R. A. Olivier, E. G. Dixon-Tulloch, P. D. Wolf, and S. Bahar, Chaos **12**, 952 (2003).
[5] K. Pyragas, Phys. Lett. A **170**, 421 (1992).
[6] J. E. S. Socolar, D. W. Sukow, and D. J. Gauthier, Phys. Rev. E **50**, 3245 (1994).
[7] J. E. S. Socolar and D. J. Gauthier, Phys. Rev. E **57**, 6589 (1998).
[8] I. Harrington and J. E. S. Socolar, Phys. Rev. E **69**, 056207 (2004).
[9] S. Bielawski, M. Bouazaoui, D. Derozier, and P. Glorieux, Phys. Rev. A **47**, 3276 (1993).
[10] A. Chang, J. C. Bienfang, G. M. Hall, J. R. Gardner, and D. J. Gauthier, Chaos **8**, 782 (1998).
[11] K. Pyragas, V. Pyragas, I. Z. Kiss, and J. L. Hudson, Phys. Rev. E **70**, 026215 (2004).
[12] W. Just, T. Bernard, M. Ostheimer, E. Reibold, and H. Benner, Phys. Rev. Lett. **78**, 203 (1997).
[13] W. Just, E. Reibold, H. Benner, K. Kacperski, P. Fronczak, and J. Holyst, Phys. Lett. A **254**, 158 (1999).
[14] K. Pyragas, Phys. Rev. E **66**, 026207 (2002).
[15] C. von Loewenich, H. Benner, and W. Just, Phys. Rev. Lett. **93**, 174101 (2004).
[16] A. G. Balanov, N. B. Janson, and E. Schöll, Phys. Rev. E **71**, 016222 (2005).
[17] K. Pyragas, Phys. Lett. A **206**, 323 (1995).
[18] A. Ahlborn and U. Parlitz, Phys. Rev. Lett. **93**, 264101 (2004).
[19] O. Beck, A. Amann, E. Schöll, J. E. S. Socolar, and W. Just, Phys. Rev. E **66**, 016213 (2002).
[20] E. M. Wright, Proc. R. Soc. Edinburgh, Sect. A: Math. Phys. Sci. **62**, 387 (1949).
[21] E. M. Wright, J. Reine Angew. Math. **194**, 66 (1955).
[22] R. Bellmann and K. L. Cooke, *Differential-Difference Equations* (Academic Press, New York, 1963).
[23] J. K. Hale, *Functional Differential Equations*, Applied Mathematical Sciences Vol. 03 (Springer, New York, 1971).
[24] F. M. Asl and A. G. Ulsoy, ASME J. Dyn. Syst., Meas., Control **125**, 215 (2003).
[25] It should be noted that a similar characteristic equation as Eq. (6) holds for the Floquet exponents of a UPO, where the lower bound, $K_{\mathrm{min}}=\lambda/2$, of the feedback gain has been shown to correspond to the flip threshold of control [12,13].
[26] W. Just, S. Popovich, A. Amann, N. Baba, and E. Schöll, Phys. Rev. E **67**, 026222 (2003).
[27] N. B. Janson, A. G. Balanov, and E. Schöll, Phys. Rev. Lett. **93**, 010601 (2004).
[28] J. N. Blakely, L. Illing, and D. J. Gauthier, Phys. Rev. Lett. **92**, 193901 (2004).
[29] D. W. Sukow, M. E. Bleich, D. J. Gauthier, and J. E. S. Socolar, Chaos **7**, 560 (1997).
[30] W. Just, D. Reckwerth, E. Reibold, and H. Benner, Phys. Rev. E **59**, 2826 (1999).
[31] P. Hövel and J. E. S. Socolar, Phys. Rev. E **68**, 036206 (2003).
[32] J. Schlesner, A. Amann, N. B. Janson, W. Just, and E. Schöll, Phys. Rev. E **68**, 066208 (2003).
[33] J. Schlesner, A. Amann, N. B. Janson, W. Just, and E. Schöll, Semicond. Sci. Technol. **19**, S34 (2004).